Macromolecules
ARTICLE

Macromolecules **2009**, *42*, 6375–6384 **6375**
DOI: 10.1021/ma9009142

Mesomorphism of Protodendritic Oligomers

Joanna Wolska,[†] Jozef Mieczkowski,[†,‡] Damian Pociecha,*[,†] Saiwan Buathong,[§] Bertrand Donnio,*[,§] Daniel Guillon,[§] and Ewa Gorecka[†]

[†]*Department of Chemistry, University of Warsaw, Al. Zwirki i Wigury 101, 02-089 Warsaw, Poland,* [‡]*Institute of Chemistry, Military University of Technology, 00-908, Warsaw, Poland, and* [§]*IPCMS, CNRS-Université de Strasbourg (UMR 7504), 23 rue du Loess, BP43, 67034, Strasbourg cedex 2, France*

Received April 27, 2009; Revised Manuscript Received July 3, 2009

ABSTRACT: New liquid-crystalline protodendritic oligomers with dimesogenic side arms are reported. These "starlike" tetrapedes were obtained by modular synthesis involving the sequential association of different anisotropic promesogenic units within the molecular architecture. This synthetic methodology allowed to prepare tetrapedal oligomers with homolithic (all identical blocks) and conjugated heterolithic (different blocks) structures. The mesomorphism was largely influenced by the peripheral aliphatic chain substitution and to a lesser extent by the chemical nature of the primary constitutive building bricks (tolane and/or stilbene fragments). Indeed, depending on the number of terminal chains grafted onto the terminal mesogens, either columnar phases, resulting from the one-dimensional stacking of supramolecular disks of ~3−6 supermolecules in fan conformation, or smectic phases, induced by the lateral two-dimensional registry of the supermolecules in cylindrical conformation, were induced. Some of the branched oligomers studied here show a rich polymorphism, a rather unusual behavior for mesogenic dendritic materials. For instance, for some of these compounds, more complex phase sequences with mesophases having long-range density modulations along the columns were also detected by small-angle X-ray diffraction studies.

Introduction

Functional liquid crystals have huge potential for applications in a wide range of scientific and technological areas, since some of the properties of the single molecules can be considerably enhanced within ordered supramolecular soft assemblies.[1−5] Controlling the self-assembling ability and the self-organizing processes of single functional moieties into periodically ordered nanostructures by molecular engineering thus remains a great and fundamental challenge in material science.[6−14] The vast majority of thermotropic mesogens possesses a simple, low-molecular-weight, molecular structure in which the rigid anisometric core, with a rodlike or disklike shape, is equipped by flexible alkyl or perfluorinated chains.[15] On the basis of such a straightforward design, nematic and smectic phases are mainly observed for the former, whereas columnar mesophases are usually formed for the latter. In recent years, there has been a growing interest in the design, synthesis, and properties of monodisperse, higher molecular weight, liquid-crystalline materials, namely oligomeric materials, with more complex and perfectly controlled molecular geometry. These supermolecules, which combine the unique physical traits of discrete low-molecular-weight materials with those of polymers, represent an attractive way of adding functionality (e.g., high control of functionality specificity and hierarchy) and to elaborate materials with tunable properties (e.g., liquid crystalline systems with low glass transition temperature, T_g) and/or with multiproperties (with cooperative and synergic effects), with potential applications in the fields of nanoscience, materials, and biology. The basic structure of supermolecules usually consists of single mesogenic or promesogenic cores linked together through flexible spacers (alkyl, siloxane chains) to generate linear oligomers (e.g., dimers, trimers, etc.)[16] or molecular structures with branched architectures[17] such as polypedes,[18−20] dendrons,[21−23] and dendrimers,[20,24] the latter having indeed proved particularly versatile candidates as novel and original scaffoldings for the elaboration of new LC functional materials. One interesting property of dendritic and prodendritic molecules is their conformational flexibility, which enables them to adopt cylindrical or disklike shapes leading to lamellar or columnar periodic self-assemblies, although in the isotropic liquid phase the molecules have a globular shape and are seemingly noncompatible for such orderings. Flexibility enables also to form columns with cross sections filled by few molecules, adopting conical or fanlike shapes.[20−24]

The most commonly studied LC dendrimers are peripherally attached end-group systems, and induction and stabilization of mesophases result from both the anisotropic interactions between the end groups, winning over the tendency of the flexible dendritic core to adopt a globular, isotropic conformation, and the microphase separation, due to the chemical and structural incompatibilities between the flexible dendritic core and the terminal groups.[24] These dendrimers adopt constrained conformational structures consequently to the occupation of specific regions by the different, incompatible, molecular parts (segmented molecular structures) in order to generate the most stable and favorable supramolecular organizations. The type of mesogen and the intrinsic connectivity (core valence, degree of branching, numbers of junctions and generations) determine the mesomorphic properties of the entire supermolecule, and all these structural parameters can be adjusted independently for an optimum control of the properties.[24] The insertion of rigid, linear branching segments within such scaffolds leads to another class of potentially interesting dendrimers referred to as main-chain systems.[25−27] Moreover, when suitably designed, such systems can possess even more complicated structures (e.g., segmented structure) forming, in some cases, uncommon mesophases.[26,27]

*Corresponding authors: Fax +33 388107246; Tel +33 3107157; e-mail pociu@chem.uw.edu.pl (D.P.), bdonnio@ipcms.u-strasbg.fr (B.D.).

Published on Web 07/20/2009

Chart 1. Chemical Structures of the Dendritic Supermolecules 20a−i[a]

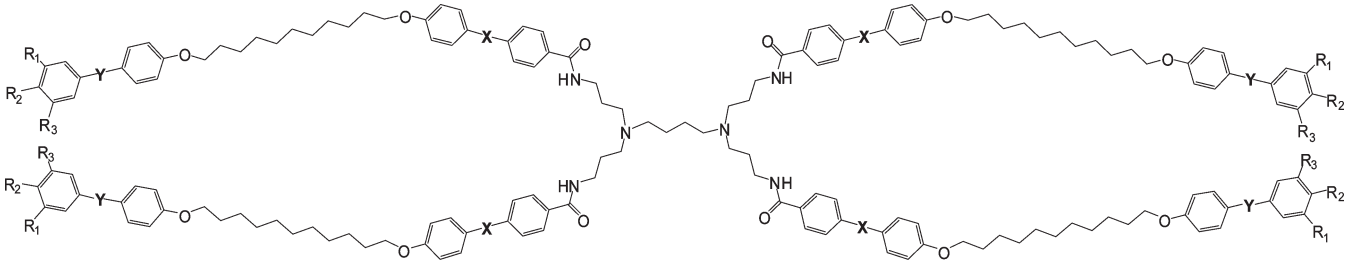

[a] **20a**: X = Y = CH=CH, $R_1 = R_2 = R_3 = OC_{12}H_{25}$; **20b**: X = CH=CH, Y = C≡C, $R_1 = R_2 = R_3 = OC_{12}H_{25}$; **20c**: X = C≡C, Y = CH=CH, $R_1 = R_2 = R_3 = OC_{12}H_{25}$; **20d**: X = Y = C≡C, $R_1 = R_2 = R_3 = OC_{12}H_{25}$; **20e**: X = Y = CH=CH, $R_1 = R_2 = OC_{12}H_{25}$, R_3 = H; **20f**: X = CH=CH, Y = C≡C, $R_1 = R_2 = OC_{12}H_{25}$, R_3 = H; **20g**: X = C≡C, Y = CH=CH, $R_1 = R_2 = OC_{12}H_{25}$, R_3 = H; **20h**: X = Y = C≡C, $R_1 = R_2 = OC_{12}H_{25}$, R_3 = H; **20i**: X = Y = C≡C, $R_2 = OC_{12}H_{25}$, $R_1 = R_3$ = H.

In the present work, we focused on a family of polypedes,[19,20] intermediate between both side-group and main-group architectures, that can be seen either as the side-chain type with dimesogenic end groups or of the main-chain one, with a degree of branching equal to unity. Three series of such dendritic systems (Chart 1) have been prepared by modular synthesis in which four mesogenic units of dimeric type were connected to the central tetravalent PPI-G0 core unit (*N*,*N*,*N*′,*N*′-tetrakis(3-aminopropyl)-1,4-butanediamine). The dimesogenic units differ in the number of terminal chains attached to the terminal phenyl ring and the place in which the double or/and triple bond was introduced into the molecular structure. The mesogenic properties of the polypedes were compared with the thermal behavior of their acid precursory branches.

Results and Discussion

Synthesis. All of the polypedes described in this article were obtained in three major steps by modular synthesis. In the first step, the internal (closer to the central core unit) and external (peripheral unit) building blocks (stilbene and acetylene moieties) of the dimeric mesogenic moieties were prepared. The internal building blocks possess an ester function, and the external ones are equipped with one or several terminal alkoxyl chains. In the second stage of the construction, these subunits were selectively coupled together through an undecyl linkage, yielding the precursory dimeric acid side arms. The final dendritic supermolecules were obtained by the coupling of the dimesogens to the tetravalent amino core (PPI-G0).

Synthesis of the Precursory Promesogenic Building Blocks. The internal stilbene subunit **6** (Scheme 1) was prepared from 4-hydroxybenzaldehyde, **1**, involving the protection of the hydroxyl group by *tert*-butyldimethylsilyl chloride (TBDMSCl) to give **2**, its conversion into the styrene **3** via the Wittig reaction, and subsequent coupling with ethyl 4-iodobenzoate by the Heck palladium-catalyzed cross-coupling reaction[28] to yield **4**. Removal of TBDMS with tetrabutylammonium fluoride (TBAF) and subsequent etherification of **5** with bromoundecanol (Mitsunobu reaction[29]) yielded the internal brick **6**. The synthesis of the analogous acetylenic derivative (Scheme 1) started from the iodoanisole (**7**), which was treated by trimethylsilylacetylene via the Sonogashira cross-coupling reaction,[28] followed by the removal of the protecting trimethylsilyl fragment (TMS, **8**) by TBAF, yielding the acetylenic derivative **9**, which was further converted by a second Sonogashira cross-coupling with 4-iodobenzoate into the tolane derivative **10**. Demethylation of **10** by BBr_3 and its conversion back to the methyl ester **11** followed by etherification with bromoundecanol yielded the internal brick **12**.

Scheme 1. Synthesis of the Internal Promesogenic Subunits 6 and 12[a]

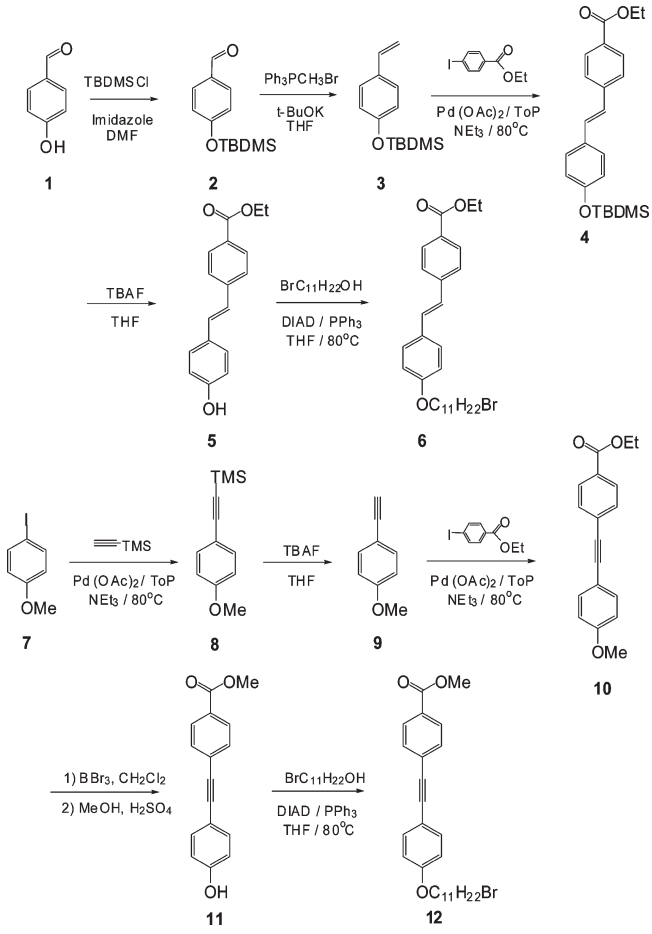

[a] Abbreviations: TBDMSCl, TMS, and TBAF are defined in the text; DMF: dimethylformamide; THF: tetrahydrofuran; DIAD: diisopropyl azodicarboxylate; ToP: tri(*o*-tolyl)phosphine.

All mono-, di-, and trialkoxy derivatives were prepared according to the same synthetic route, shown in Scheme 2, starting from the appropriate alkoxybenzaldehydes (**13i**−**iii**).[26] In one case, benzaldehydes **13i**−**iii** were transformed into their styrene homologues **14i**−**iii** via the Wittig reaction, and their subsequent coupling with iodophenol by the palladium-catalyzed Heck reaction led to the stilbene derivatives **15i**−**iii**. In the other case, the benzaldehydes **13i**−**iii** were converted into dibromo vinylic derivatives **16i**−**iii** by the Corey−Fuchs procedure[30] and transformed by dehydrohalogenation into the terminal alkyne derivatives **17i**−**iii** by treatment with lithium diisopropylamide (LDA, Scheme 2). Compounds **17i**−**iii** were then coupled with iodophenol via

Sonogashira cross-coupling to yield the peripheral tolane subunits **18i−iii**.

Synthesis of the Acid Side Arms and Polypedes. All the dimeric acids **19a−i** were obtained via Williamson etherification between the appropriate internal subunits derivatives (**6** and/or **12**) and the library of external building blocks, **15i−iii** and/or **18i−iii**, followed by the hydrolysis of the dimeric ester arms (Scheme 3). The final dendritic compounds, **20a−i**, were obtained through the acylation reaction (Scheme 3) between the appropriate acid precursors (**19a−i**) and the tetraamino core (PPI-G0) in the presence of benzotriazol-1-yloxy-tris(dimethylamino)phosphonium hexafluorophosphate (Castro reagent or BOP).

Synthesis of the Monomeric Type Oligomers. The branches of "short" dendrimers, **24a,b**, were obtained in a similar way as the external building blocks **15i−iii**. The aldehydes **21a,b** were converted into the vinylic derivatives **22a**,**b** via Wittig reaction and coupled with ethyl 4-iodobenzoate to yield **23a**,**b**. The ester derivatives were hydrolyzed into the carboxylic acids **24a**,**b**, which were further used in acylation reaction with PPI-G0 to yield the "short" dendrimers **25a**,**b** (Scheme 4).

Scheme 2. Synthesis of the External Stilbene (15i−iii) and Tolane (18i−iii) Subunits

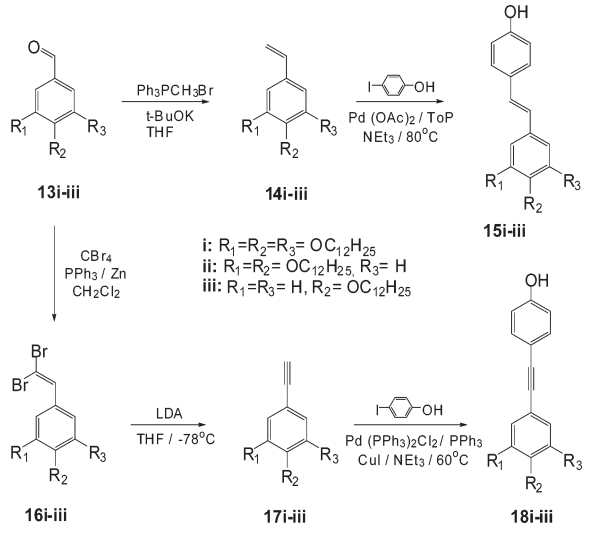

Mesomorphic Properties. All the studied dendritic supermolecules and their corresponding acid precursors are mesomorphic, and the morphology of the mesophases is governed by the number of alkyl chains grafted on the peripheral mesogenic groups. The two compounds of series **3** with one terminal chain per end-mesogenic unit (**19i**, **20i**) form exclusively smectic phases, whereas all members of series **1** (**19a−d**, **20a−d**) and series **2** (**19e−h**, **20e−h**), bearing three and two terminal chains per end-mesogenic unit, respectively, form predominantly columnar phases; most of them consist of a hexagonal arrangement of the columns (Table 1), although for some compounds (**19b−d**, **20d**, **20h**) below the hexagonal phase, more structurally complex phases were detected, with rectangular or oblique 2D symmetries or with a modulation of the electron density along the columnar axis (pseudo-3D phases).

All the mesophases can be considered as disordered, as they show only one broad and diffuse signal in the wide-angle region of the X-ray diffraction (XRD) patterns, centered at around 4.5 Å, distance reflecting the liquidlike state of the molten alkyl chains. In the low-angle region, sharp signals reflecting the 2D arrangement of the columns (series **1** and **2**) or the 1D lamellar structures (series **3**) were detected. It was found that the relative positions of the ethylene and acetylene linkages within the arms have a minor influence on the phase sequence and nature but in conjunction with chain numbers affect singularly the transition temperatures and phases' parameters within each series. The intermolecular distances (column diameter, a, or smectic layer thickness, d) are strongly dependent on the total number of terminal chains grafted on the supermolecule: the larger the terminal chains number, the shorter the mesophase periodicity (Figure 1); this aspect will be discussed thereafter. The precursory acid compounds form columns/layers with similar dimensions to that of the related dendritic homologues. Assuming a density

Scheme 3. Synthesis of the Acid Arms (19a−i) and Polypedes (20a−i)[a]

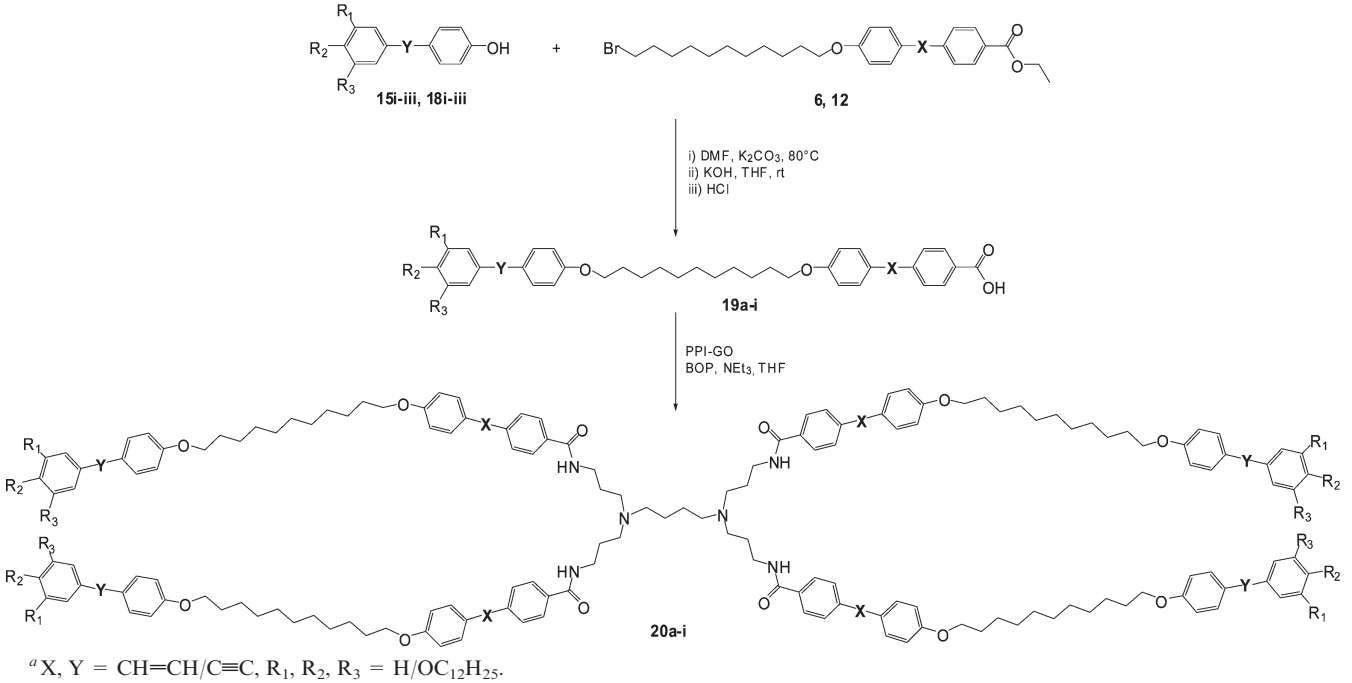

[a] X, Y = CH=CH/C≡C, R_1, R_2, R_3 = H/$OC_{12}H_{25}$.

Scheme 4. Synthesis of the "Short" Dendrimers 25a (Z = H) and 25b (Z = NO_2)

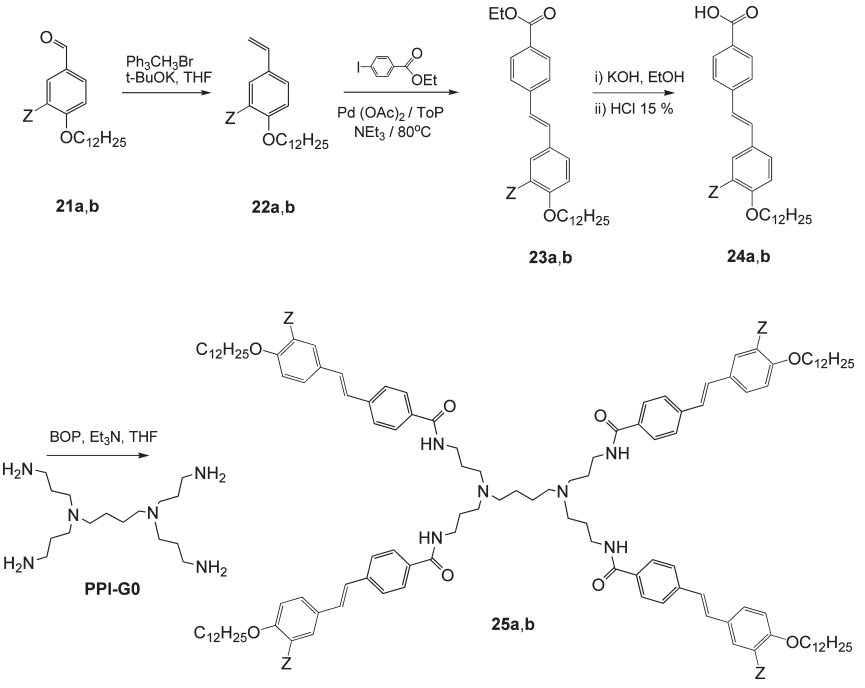

of 1 g cm^{-3} and that the thickness of an elementary columnar slice for the columnar phases is $h \sim 4.5$ Å, it is possible to estimate the number of polypedes (N_{dend}), likely in a folded fan conformation, number of acidic arms (N_{ac}), and number of mesogens (N_{mes}) that self-associate within the column cross section (Figure 2), according to $N_{dend/ac} = Sh/V_{dend/ac}$ ($V_{dend/ac}$: molecular volume).[31] For series **1**, it was found that 3.5−4 supermolecules per such defined columnar slice, that is, around 30 mesogenic cores ($28 < N_{mes} < 32$), are necessary to fulfill the volume requirements, also in perfect agreement with the number of acid precursors self-associating in columnar phases ($N_{ac} = 14-15$ molecules, i.e., $N_{mes} = 28-30$). For series **2**, these numbers increase slightly ($N_{dend} \sim 5-6$, $N_{ac} \sim 20-24$, $N_{mes} \sim 40-48$) since the lattice parameters are greater than those of series **1** (Table 1), but still with the same accordance between acids and dendrimers numbers. In both series, the chemical structure of the oligomers (disposition of the stilbenoid-like and tolanoid-like segments) does not influence this arrangement greatly, suggesting a less efficient microsegregation between the various segments, contrasting to what was observed in the related octopus dendrimers (Figure 2).[26] Finally, the total numbers of peripheral alkyl chains irradiating from the columnar interface are similar (ca. 40−48 chains) in both series **1** and **2**, further emphasizing the single mode of packing of the polypedes and arms into columns.

Finally, as for the two compounds of series **3** (**19i**, **20i**), both the acid and the oligomeric compounds exhibit smectic phases as expected for dendrimers bearing one chain per mesogenic end group.[20,24] The determination of the molecular area ($A_{mol} = V_{mol}/d$), directly deduced from the molecular volume and the layer periodicity, gives values (30 $Å^2$ for **19i** and 54 $Å^2$ for **20i**) that are compatible with an elongated prolate conformation for the acidic arm and the polypede, where the rigid parts are quasi-collinear to the layer normal, required for the formation of the lamellar mesophases (Figure 2). In the case of the compound **19i**, formation of a dense dynamic H-bonding 2D network between neighbored acids is likely (head-to-head disposition), helping stabilizing their organization into layer, with two successive rows of mesogenic groups on either side of this central slab. The values of the molecular area and lamellar periodicities (quasi-constant throughout the mesomorphic temperature domain) compared to the molecular length suggest a tilt of the mesogenic groups, and therefore tilted smectic mesophases (SmJ, SmI, SmC),[32] in agreement with the POM observations. Similarly, the dendritic oligomer adopts a prolate conformation (giant cylinder) with the mesogenic units (i.e., eight in the present case) distributed homogeneously on either sides of the molecular center and the formation of the smectic lamellar phases results from their parallel disposition (Figure 2); the value of the molecular area (27 $Å^2$ per end group) is fully consistent with an orthognal-like smectic phase, i.e., SmA phase.[26]

The "short" G0 dendrimers **25a** and **25b** with monomeric type mesogenic units form exclusively lamellar phase (SmA) with high clearing temperatures. Their molecular arrangements are similar in both cases and consist of the lateral packing of the dendrimers in an elongated conformation,[20] with the tetravalent cores located in the central slab of the smectic layer, as confirmed by their molecular areas (61 and 65 $Å^2$, respectively).

The isotropization temperatures for the acid precursors are usually higher than for the corresponding dendritic compounds. This indicates that while in the case of polypedes the columns are formed by the self-assembling of a few molecules, in a folded fanlike conformation, interacting through weak van der Waals forces, the acid molecules forming columns are connected by stronger hydrogen bonds instead. The difference in clearing temperatures between the acid and the tetrapede is even stronger in the case of compounds of series **3** exhibiting lamellar phases. The importance of hydrogen bonding is also reflected by the fact that the conversion of the acid precursor into the ethyl ester resulted in a nonmesogenic material (e.g., ethyl ester of compound **19f** exhibits direct transition from crystalline to isotropic liquid at 120 °C and recrystallizes at 95 °C).

Thus, many properties of the here-described materials are consistent with those observed previously for other dendrimeric mesogens.[20,24] The change in the number of terminal

Table 1. Phase Sequence, Phase Transition Temperatures, and Enthalpy Changes for Studied Compound as Well as Structural Data Obtained from X-ray Diffraction Studies[a]

	X	Y	R_1	R_2	R_3	phase sequence[b]	crystallographic data[d]
						Series 1	
19a	CH=CH	CH=CH	$OC_{12}H_{25}$	$OC_{12}H_{25}$	$OC_{12}H_{25}$	Cr 83.6 (10.9) Col_{ph} 190 (−) I	a = 83.7 Å at 180 °C
19b	CH=CH	C≡C	$OC_{12}H_{25}$	$OC_{12}H_{25}$	$OC_{12}H_{25}$	Cr 93 Col_r 111.9 (1.7) Col_h ~140 Col_{ph} > 190 I[c]	a = 89.9 Å at 150 °C a = 77.2 Å at 135 °C a = 87.1 Å, b = 135.3 Å, γ = 90° at 100 °C
19c	C≡C	CH=CH	$OC_{12}H_{25}$	$OC_{12}H_{25}$	$OC_{12}H_{25}$	Cr 90 Col_o 123.9 (4.7) Col_{ph} 162.7 (6.9) I[c]	a = 84.6 Å at 130 °C a = 62.4 Å, b = 177.7 Å, γ = 84.7° at 120 °C
19d	C≡C	C≡C	$OC_{12}H_{25}$	$OC_{12}H_{25}$	$OC_{12}H_{25}$	Cr 42.6 (17.2) Col_o 127.6 (7.6) Col_{ph} 174.8 (12.6) I	a = 83.0 Å at 170 °C a = 62.7 Å, b = 172.2 Å, γ = 92.6° at 100 °C
20a	CH=CH	CH=CH	$OC_{12}H_{25}$	$OC_{12}H_{25}$	$OC_{12}H_{25}$	Cr 55 Col_h 170 I[c]	a = 79.1 Å at 130 °C
20b	CH=CH	C≡C	$OC_{12}H_{25}$	$OC_{12}H_{25}$	$OC_{12}H_{25}$	Cr 112.1 Col_h 156.7 (9.6) I[c]	a = 92.6 Å at 125 °C
20c	C≡C	CH=CH	$OC_{12}H_{25}$	$OC_{12}H_{25}$	$OC_{12}H_{25}$	Cr 127.2 (7.6) Col_h 163.2 (0.2) I	a = 82.8 Å at 136 °C
20d	C≡C	C≡C	$OC_{12}H_{25}$	$OC_{12}H_{25}$	$OC_{12}H_{25}$	Cr 129.8 (3.1) [Col_h modulated 106.2 (0.3)] Col_h 166.4 (1.6) I	a = 82.2 Å at 155 °C
						Series 2	
19e	CH=CH	CH=CH	$OC_{12}H_{25}$	$OC_{12}H_{25}$	H	Cr 154.8 (22.9) Col_h 188.5 (0.5) I	a = 100 Å at 160 °C
19f	CH=CH	C≡C	$OC_{12}H_{25}$	$OC_{12}H_{25}$	H	Cr 140 Col_h > 200 I[c]	a = 94.4 Å at 150 °C
19g	C≡C	CH=CH	$OC_{12}H_{25}$	$OC_{12}H_{25}$	H	Cr 164.4 (45.2) Col_h 199.8 (21.6) I	a = 93.3 Å at 195 °C
19h	C≡C	C≡C	$OC_{12}H_{25}$	$OC_{12}H_{25}$	H	Cr 160.2 (16.6) Col_h 198.4 (18.6) I	a = 89.7 Å at 160 °C
20e	CH=CH	CH=CH	$OC_{12}H_{25}$	$OC_{12}H_{25}$	H	Cr 185 Col_h 195 I[c]	a = 92.8 Å at 190 °C
20f	CH=CH	C≡C	$OC_{12}H_{25}$	$OC_{12}H_{25}$	H	Cr 106 Col_h 152.7 (7.2) I[c]	a = 93.7 Å at 135 °C
20g	C≡C	CH=CH	$OC_{12}H_{25}$	$OC_{12}H_{25}$	H	Cr 118.0 (13.3) Col_h 151.8 (3.0) I	a = 102.2 Å at 130 °C
20h	C≡C	C≡C	$OC_{12}H_{25}$	$OC_{12}H_{25}$	H	Cr 122.7 (14.8) Col_r modulated 143.9 (0.2) Col_h 165.9 (0.8) I	a = 95.4 Å at 145 °C a = 230 Å, b = 94 Å, c = 180 Å[e] at 126 °C
						Series 3	
19i	C≡C	C≡C	H	$OC_{12}H_{25}$	H	Cr 189.0 (10.8) SmJ 205.0 (2.1) SmI 210.4 (2.2) SmC 226.3 (0.8) I	d = 86.4 Å at 200 °C
20i	C≡C	C≡C	H	$OC_{12}H_{25}$	H	Cr 155.4 (30.6) SmA 197.0 (15.2) I	d = 103.2 Å at 190 °C
						"Short" Dendrimers	
25a						Cr 150 SmA > 250 I[c]	d = 50.9 Å at 170 °C
25b						Cr 120 SmA > 210 I[c]	d = 52.7 Å at 200 °C

[a] a, b, and γ: lattice parameters of the 2D cells of the columnar phases and angle between a and b; d: periodicity of the smectic phases. [b] Abbreviations: Cr: crystalline phase, Col_h and Col_{ph}: columnar hexagonal phases; Col_r: columnar rectangular phase; Col_o: oblique columnar phase; SmJ: smectic J phase; SmI: smectic I phase; SmC: smectic C phase; SmA: smectic A phase; I: isotropic liquid. [c] For some phase transitions, the DSC signal was very broad or too weak, preventing to obtain reliable data, in such case transition temperature is taken from microscopic and X-ray studies. When measurable, enthalpy of transition, ΔH, is given in brackets (in J g^{-1}). [d] All phases above crystalline phase show diffused signal centered at 4.5 Å corresponding to average distance between molten of alkyl chains. For columnar hexagonal phases Col_h and Col_{ph} the primitive cell parameter is given, while for rectangular Col_r and oblique Col_o phase the 2D centered cell was chosen. [e] Because of the limited number of observed X-ray signals and poor alignment of the cell, only a rough estimation of cell unit diameter is possible.

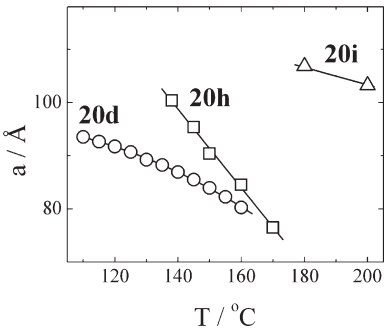

Figure 1. Intermolecular distances vs temperature for dendritic compounds **20d** and **20h** (○, □: columnar diameter, *a*) and **20i** (△: layer spacing, *d*); see Scheme 3 for the molecular structures.

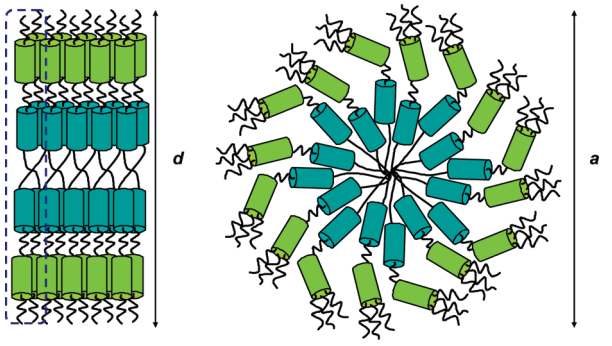

Figure 2. Proposed schematic representation of the organization of the polypedal oligomers in smectic (side view) and columnar phases (top view).

chains per end group modifies the relationships between the hard and the soft parts, and consequently the molecules adopt either a parallel (prolate, series **3**) or a flat (oblate, series **1** and **2**) conformation, and smectic and/or columnar mesophases are induced, respectively (Figure 2). Compounds with only one terminal chain per end group (series **3**), for which the compatibility of spatial requirement between the alkyl chains and mesogenic cores is satisfied, self-organize into noncurved smectic layers. In contrast, the grafting of additional terminal chains at the extremity of the outer tolane or stilbene part prevents such a parallel disposition of the promesogenic groups, since the cross-sectional area of the terminal chains is larger than the area occupied by the mesogenic units (the mismatch between the surface areas of the aromatic cores and the cross section of the aliphatic chains results in the curvature of all the interfaces); they are forced to be radially arranged around the central moiety, and the dendritic oligomers adopt a fanlike conformation. Consequently, compounds of series **1** and **2** exhibit columnar phases in which the column cross section is made of a few molecules. In order to pack efficiently, molecules most probably adopted strongly bent conformation, allowed by virtue of their great flexibility. The protodendrimers and their acid precursors have similar mesophase behavior, showing that the column structure is determined mainly by the tendency to separate mesogenic cores and alkyl chains, while the type of bonds joining the mesogenic cores that are chemical bonds (dendrimers) or hydrogen bonds (acid precursors) has only a minor effect. The column diameter is determined by the number of terminal alkyl chains. For larger number of chains higher curvature of the surface separating mesogenic cores and melted terminal chains is necessary, which is realized by reducing the diameter of the column.

The effect of the degree of branching on the properties can be evaluated by comparing the thermal behavior of the polypedes **20** and the precursor acids **19**, having a degree of branching, $N_B = 1$, with that of the homologous octopus dendrimers **27** and their related acid parents **26** having a branching degree of 2 ($N_B = 2$, Scheme 5), reported previously.[26] In all cases increasing the degree of branching results in mesophases destabilization, likely due to more steric packing constraints: some of the branched acids **26** were not mesogenic, and clearing temperatures of all octopus dendrimers **27** were lower than the corresponding compounds **20** (see phase diagrams in the Supporting Information for comparison). The reduction of the degree of branching ($N_B = 1$), and thus the higher conformational freedom, is likely responsible for the loss of segregation between the constituting segments inside the column cores, as is the case for the octopus dendrimers.

X-ray Diffraction Studies. *Series 1.* All dendritic oligomers of series **1** (**20a**−**d**, Table 1) form exclusively a hexagonal columnar phase (*p6mm*[33] Col_h) above a crystalline or glassy solid. For **20d**, however, a monotropic columnar phase is found below the Col_h phase, characterized by XRD with the presence of additional peaks, incommensurate with those associated with the hexagonal structure. The position of these supplementary signals in the XRD pattern of a partially aligned sample shows that the signals may be attributed to some electron density modulations along the columns, with a period of about 120 Å. It is possible that such modulations are induced by helical arrangement of the dendritic molecules assembled into columns[34] or due to undulation of the columns.[35] The phase sequences for the acid precursors of series **1** (**19a**−**d**, Table 1) are more complex. The X-ray data indicate formation of the hexagonal columnar phase below the isotropic liquid; however, the optical textures, in particular the shape of the liquid crystalline germs growing from the isotropic phase (Figure 3a), and lack of nonbirefringent regions in the texture (remaining dark under rotation between crossed polarizers, Figure 3b) suggest that the phase is pseudohexagonal (Col_{ph}), with a phase symmetry lower than *p6mm*. One possible explanation is that the 2D hexagonal Bravais[33] lattice is formed "accidentally", and it is filled with columns of noncircular cross sections (elliptical cross section with random in-plane orientations of the two main axes).[36]

Below the pseudohexagonal columnar phase (**19c** and **19d**), a columnar phase with slightly oblique, centered crystallographic unit cell, is formed, in which the distortion of the cell from hexagonality is rather strong (Figure 4). The distortion can be quantified comparing the ratio of the centered crystallographic unit cell sides' dimensions in the Col_o phase, $b/a \sim 3$ with that of the Col_h phase, $b/a = \sqrt{3}$. Analysis of the XRD signal intensities in the Col_o phase (intensities of signals (20) and (11) are nearly equal but only half the intensity of the −11 reflection) shows that the phase structure is different than a simply distorted hexagonal lattice. Hexagonal or rectangular phases are usually pictured as being made of columns with centers of high electron density, in which aromatic molecular cores are collected, homogenously surrounded by lower electron density areas, in which alkyl chains are collected.[37] The electron density map of Col_o phase (Figure 4) shows that the aromatic part of the columnar cross section becomes oblate, and alkyl chains are collected mainly below and above this region, giving rise to the partial layering of the structure. Thus, the structure reminds the ribbon type phase. In compounds **19c** and **19d**, the phase transition between pseudohexagonal and oblique columnar phase is first order and accompanied by clear optical changes—in the Col_o phase the birefringence strongly increases (Figure 3c). Even more complicated is the

temperature phase sequence observed for compound **19b,** in which two mesophases with hexagonal lattice symmetry are observed above the rectangular columnar phase (Figure 4). In this case, the lattice ratio $b/a \sim 1.9$ of the rectangular phase only slightly deviates from the hexagonal one. Moreover, the phase transitions in this compound are observed only by some changes in the X-ray pattern, the optical textures remaining in all phases a low birefringent mosaic type, similar to that observed in the pseudohexagonal columnar phase. There is no direct hint what differentiates both the hexagonal columnar structures; most probably, they differ only slightly in the column cross-section shape (elliptical versus circular, with random orientation).

Series 2. The polypedes of series **2** (**20e**−**h**, Table 1) show predominantly a hexagonal columnar phase. The exception is compound **20h**, for which on lowering the temperature a sequence Col_h−Col_r is observed. This transition is accompanied by the increase of the birefringence in the rectangular

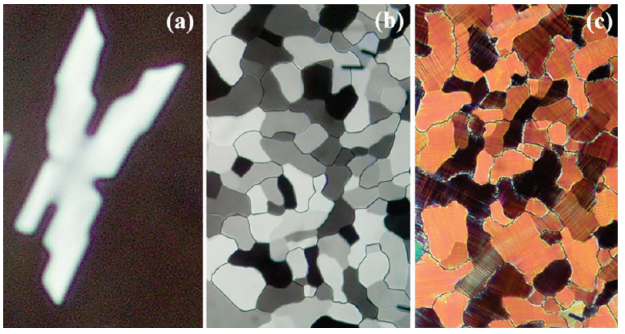

Figure 3. (a) Liquid-crystalline germ growing from isotropic phase (T = 160 °C), (b) mosaic texture of columnar pseudohexagonal phase (T = 135 °C), and (c) mosaic texture of oblique columnar phase for compound **19c** (T = 115 °C); see Scheme 3 for the molecular structure.

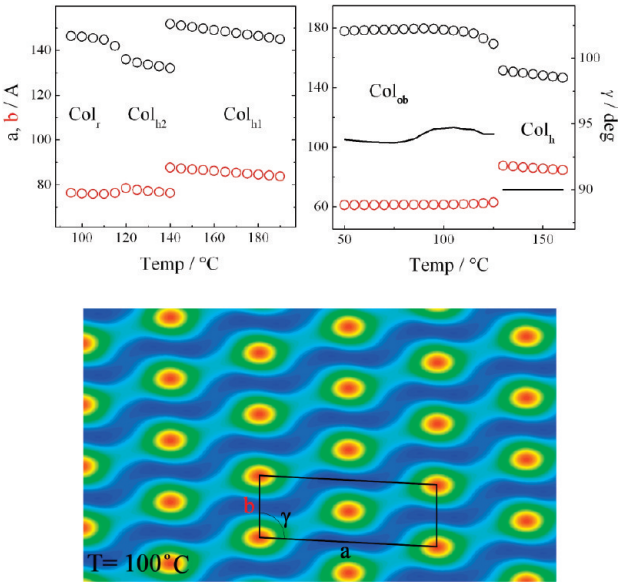

Figure 4. Top: temperature dependence of the crystallographic unit cell parameters for compounds **19b** (left) and **19c** (right); see Scheme 3 for the molecular structure. In all phases the centered unit cell was chosen to show readily the evolution of the crystallographic structure (for Col_h phase $b/a = \sqrt{3}$). Bottom: electron density map in the plane perpendicular to the column axis for compound **19c** in the columnar oblique Col_o phase. Map was obtained by the reversed Fourier transform, the structure factor amplitudes were taken as a square root of signal intensities, and all structure factors were taken positive. Blue and red are regions of lowest and highest electron density, corresponding to high concentration of aromatic or alkyl parts of molecules, respectively.

Scheme 5. Structure of the Octopus Dendrimers 27 with Degree of Branching N_B = 2, Reported in Ref 26 **(X, Y = CH=CH/C≡C, R_1, R_2, R_3 = H/$OC_{12}H_{25}$)**

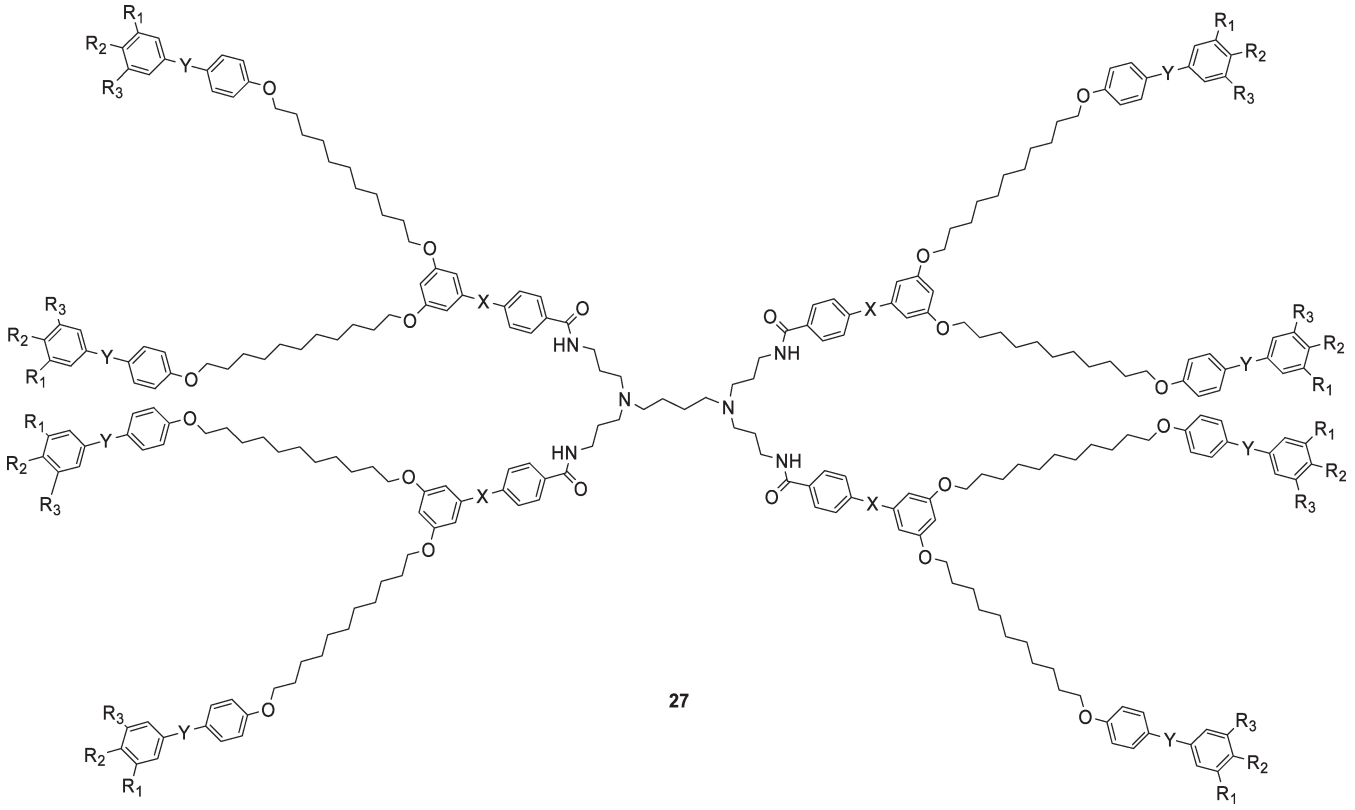

27

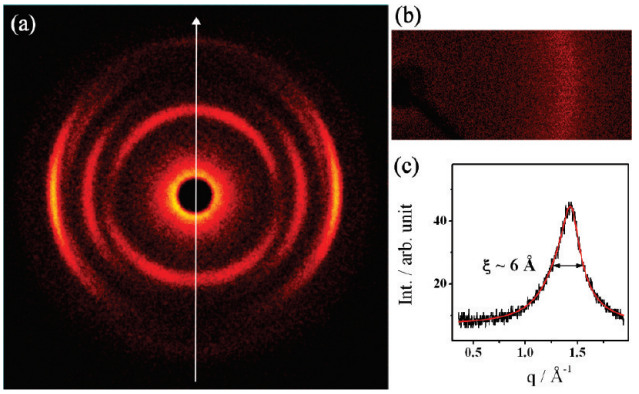

Figure 5. Low (a) and wide (b) angle X-ray diffraction pattern for partially aligned sample of material **20h** (see Scheme 3 for the molecular structure) at 130 °C; arrow in (a) indicates column axes direction. Existence of nonequatorial signals (not perpendicular to column axis direction) proves modulation in the column structure. (c) Integrated intensity from pattern (b) vs wavevector q. The signal is centered at 4.4 Å, and the correlation length obtained from the signal width at half-maximum is ~6 Å.

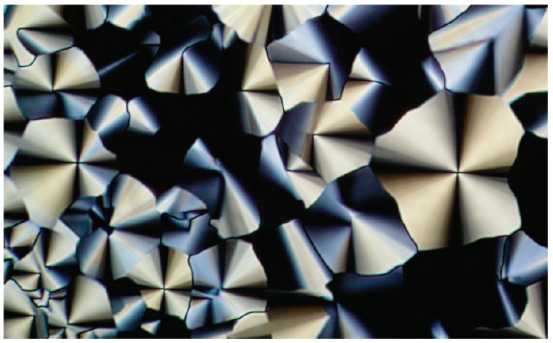

Figure 6. Texture of the hexagonal columnar Col_h phase of compound **19g** (T = 185 °C); see Scheme 3 for the molecular structure.

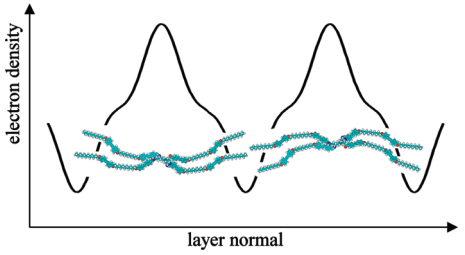

Figure 7. Schematic drawing of electron density profile along the smectic layer normal obtained for compound **20i** (see Scheme 3 for the molecular structure); enhanced electron density in the layer corresponds to the regions filled either with dendrimeric scaffold and/or with the mesogenic cores.

phase and changes in the small angle region of the X-ray pattern. The low-angle X-ray pattern for a partially aligned sample (Figure 5) shows that the actual structure of the columnar phase is 3D, with long-range periodicity (~200 Å that corresponds to about 45 supramolecular disks) along the columns. It can be excluded that this long periodicity along the column is due to the helix formed by slow rotation of the disks around the column axis. Rectangular lattice of columns imposes that the column cross sections have to generate an elliptical shape, while such rotation would impose an overall circular cross section of the columns. Elliptical projection could be however preserved if the helix is obtained by rotation of tilted disks around their short axis. Another possibility is that the modulation of the electron density along the column is due to columns undulations or slow oscillations of the elliptical disks along the columnar axis.

All the acid precursors of this series **2** (**19e**−**h**, Table 1) form exclusively a hexagonal columnar phase (Figure 6).

Series 3. Oligomer **20i** and its acid precursor **19i**, with one terminal alkyl chain, exhibit lamellar phases in a broad temperature range. By analyzing relative intensities of consecutive harmonics of the main signal in X-ray pattern of compound **20i** (the second harmonic is extinguished and third harmonic is ~1/15 of the main signal intensity), an unusual electron density profile along the layer normal can be deduced, which is however consistent with the molecular structure of the compound (Figure 7).

Conclusions

New liquid-crystalline protodendritic oligomers with dimesogenic side arms have been synthesized. Their mesomorphic properties were largely influenced by the peripheral aliphatic chain substitution and to a lesser extent by the chemical architecture, and either columnar or smectic mesophases were induced.

Some of the compounds studied here show a rich polymorphism, a rather unusual behavior for mesogenic macromolecules. In particular, two materials form mesophases with three-dimensional structures, but with liquidlike short-range order within the columns. Such 3D structure is usually attributed to helical arrangement of the molecules in the column. The corresponding acid precursors form frequently, apart for a hexagonal columnar phase, also mesophases with rectangular or oblique crystallographic lattices. For the latter case obtained electron density maps suggest some layering of the structure achieved by deformation of column cross section from circular shape and partial connection between neighboring columns.

Experimental Section

The preparation of the dendrimers and their analytical and spectroscopic data are given thereafter; the preparation of all the precursory compounds is described in the Supporting Information. Since all of the dendrimers were prepared accordingly, the preparation of **20a** was chosen as a representative example and is shown below.

Into a solution of compound **19a** (0.25 g, 0.219 mmol), PPI-G0 (0.017 g, 0.548 mmol), and NEt_3 (2 mL, 14 mmol), in DMF, BOP (0.1 g, 0.236 mmol) was added. The mixture was stirred for 2 h at 55 °C and then poured into water, and the solid was filtrated. The crude product was dissolved in $CHCl_3$ and the organic layer thoroughly washed with water and dried over $MgSO_4$. The final compound was purified by column chromatography on silica gel ($CHCl_3$) and precipitated with MeOH to yield product **20a** (0.12 g, 46%). For all the final compounds, the four amidic protons were not detected.

20a. ^{1}H NMR (300 MHz, $CDCl_3$), δ [ppm]: 7.73 (d; J^3 = 8.0 Hz; 8H); 7.47−7.37 (m; 28H); 7.33 (d; J^3 = 16.4 Hz; 4H); 7.04 (d; J^3 = 16.2 Hz; 4H); 6.98 (m; 20H); 6.68 (s; 8H); 4.08−3.83 (m; 40H); 3.58−3.39 (m; 8H); 2.66−2.30 (m; 12H); 1.88−1.68 (m; 40H); 1.55−1.16 (m; 284H); 0.89 (t; J^3 = 6.8 Hz; 36H). ^{13}C NMR (75 MHz; $CDCl_3$), δ [ppm]: 167.30; 159.24; 158.77; 153.38; 152.69; 140.62; 138.00; 132.91; 130.11; 130.00; 129,40; 129,34; 128.00; 127.52; 127.49; 127.32; 126.69; 126.12; 125.19; 114.72; 114.68; 113.98; 107.29; 104.98; 73.54; 69.19; 68.06; 31.93; 30.36; 29.77; 29.71; 29.67; 29.58; 29.44; 29.40; 29.37; 29.32; 26.14; 26.08; 22.70; 14.12. M_{calc} = 4810.80 g mol^{-1} (100%) for $C_{320}H_{496}N_6O_{24}$; MS = 4811.36 g mol^{-1}.

20b. ^{1}H NMR (300 MHz, $CDCl_3$), δ [ppm]: 7.73 (d; J^3 = 8.3 Hz; 8H); 7.48−7.38 (m; 16H); 7.36 (d; J^3 = 9.0 Hz; 8H); 7.02(d; J^3 = 16.2 Hz; 4H); 6.89 (d; J^3 = 16.2 Hz; 4H); 6.86 (d; J^3 = 9.0 Hz; 8H);

6.83 (d; $J^3 = 9.0$ Hz; 8H); 6.71 (s; 8H); 4.04(m; 40H); 3.57−3.42 (m; 8H); 2.58−2.33 (m; 12H); 1.87−1.70 (m; 40H); 1.53−1.41 (m; 40H); 1.40−1.20 (m; 244H); 0.88 (t; $J^3 = 6.8$ Hz; 36H). ^{13}C NMR (75 MHz; $CDCl_3$), δ [ppm]: 167.31; 159.23; 159.13; 152.98; 140.59; 138.84; 132.93; 130.16; 130.09; 129.34; 128.87; 128.00; 127.51; 127.04; 126.11; 125.20; 118.03; 115.20; 114.72; 114.36; 110.02; 88.32; 88.14; 73.52; 69.12; 68.06; 53.96; 52.36; 39.09; 31.94; 30.34; 30.15; 29.77; 29.71; 29.66; 29.62; 29.58; 29.47; 29.40; 29.38; 29.34; 26.10; 22.70; 14.12. $M_{calc} = 4802.73$ g mol^{-1} (100%) for $C_{320}H_{488}N_6O_{24}$; MS = 4824.22 g mol^{-1}.

20c. ^{1}H NMR (500 MHz, $CDCl_3$), δ [ppm]: 7.77 (d; $J^3 = 8.0$ Hz; 8H); 7.49 (d; $J^3 = 8.1$ Hz; 8H); 7.42 (d; $J^3 = 8.7$ Hz; 8H); 7.40 (d; $J^3 = 8.7$ Hz; 8H); 6.91 (d; $J^3 = 16.2$ Hz; 4H); 6.89−6.78 (m; 20H); 6.68 (s; 8H); 4.05−3.89 (m; 40H); 3.56−3.43 (m; 8H); 2.75−2.20 (m; 12H); 1.85−1.63 (m; 40H); 1.58−1.41 (m; 40H); 1.40−1.18 (m; 244H); 0.88 (t; $J^3 = 7.0$ Hz; 36H). ^{13}C NMR (125 MHz; $CDCl_3$), δ [ppm]: 159.58; 158.81; 153.32; 152.73; 138.15; 133.22; 132.95; 131.47; 130.08; 129.41; 127.54; 127.37; 126.74; 114.76; 114.63; 114.03; 105.12; 92.02; 87.43; 73.56; 73.50; 69.26; 68.12; 31.96; 30.38; 29.77; 29.72; 29.68; 29.51; 29.46; 29.38; 26.17; 26.09; 22.70; 14.11. $M_{calc} = 4802.73$ g mol^{-1} (100%) for $C_{320}H_{488}N_6O_{24}$; MS = 4816.52 g mol^{-1}.

20d. ^{1}H NMR (200 MHz, $CDCl_3$), δ [ppm]: 7.77 (d; $J^3 = 8.1$ Hz; 8H); 7.49 (d; $J^3 = 8.4$ Hz; 8H); 7.46−7.35 (m; 16H); 6.85 (d; $J^3 = 8.8$ Hz; 8H); 6.83 (d; $J^3 = 9.0$ Hz; 8H); 6.70 (s; 8H); 4.08−3.83 (m; 40H); 3.64−3.36 (m; 8H); 2.70−2.32 (m; 12H); 1.92−1.63 (m; 40H); 1.59−1.06 (m; 284H); 0.88 (t; $J^3 = 678$ Hz; 36H). ^{13}C NMR (50 MHz; $CDCl_3$), δ [ppm]: 167.24; 159.70; 159.30; 153.15; 138.96; 133.40; 133.12; 131.62; 127.27; 118.20; 115.36; 114.76; 114.69; 110.13; 92.20; 88.49; 88.32; 87.61; 73.71; 69.29; 68.25; 32.12; 30.51; 29.90; 29.84; 29.76; 29.60; 29.42; 26.29; 22.90; 14.32. $M_{calc} = 4794.66$ g mol^{-1} (100%) for $C_{320}H_{480}N_6O_{24}$; MS = 4799.86 g mol^{-1}.

20e. ^{1}H NMR (200 MHz, $CDCl_3$), δ [ppm]: 7.92 (d; $J^3 = 8.3$ Hz; 8H); 7.76 (d; $J^3 = 8.2$ Hz; 8H); 7.52−7.18 (m; 24H); 7.12 (d; $J^3 = 16.1$ Hz; 4H); 7.09−6.32 (m; 32H); 4.12−3.91 (m; 32H); 3.63−3.31 (m; 8H); 2.63−2.41 (m; 12H); 1.92−1.59 (m; 32H); 1.56−1.02 (m; 212H); 0.99−0.72 (m; 24H). ^{13}C NMR (50 MHz; $CDCl_3$), δ [ppm]: 169.28; 158.97; 158.64; 155.62; 141.34; 139.11; 133.89; 131.23; 131.33; 130.62; 130.24; 129.54; 128.68; 128.51; 128.41; 127.63; 127.24; 126.67; 115.69; 115.34; 114.86; 109.42; 105.96; 72.57; 70.84; 69.86; 31.86; 30.47; 29.98; 29.87; 29.74; 29.63; 29.57; 29.51; 29.42; 29.39; 26.28; 22.63; 14.25. $M_{calc} = 4074.06$ g mol^{-1} (100%) for $C_{272}H_{400}N_6O_{20}$; MS = 4080.26 g mol^{-1}.

20f. ^{1}H NMR (500 MHz, $CDCl_3$), δ [ppm]: 7.71 (d; $J^3 = 7.8$ Hz; 8H); 7.45−7.32 (m; 24H); 7.31 (dd; $J^4 = 2.0$ Hz; $J^3 = 8.2$ Hz; 4H); 7.20(d; $J^3 = 16.0$ Hz; 4H); 6.95−6.74 (m; 24H); 6.66 (d; $J^3 = 8.2$ Hz; 4H); 4.07 (m; 32H); 3.57−3.37 (m; 8H); 2.57−2.43 (m; 8H); 2.42−2.33 (m; 4H); 1.85−1.66 (m; 32H); 1.50−1.04 (m; 212H); 0.93−078 (m; 24H). ^{13}C NMR (125 MHz; $CDCl_3$), δ [ppm]: 167.50; 159.48; 159.22; 158.55; 149.82; 149.02; 140.84; 133.16; 133.06; 130.34; 130.14; 128.21; 127.70; 126.33; 125.43; 122.30; 116.97; 114.96; 114.67; 114.40; 88.41; 87.98; 69.42; 69.33; 68.27; 53.01; 52.62; 39.33; 32.13; 29.90; 29.87; 29.83; 29.64; 29.57; 29.53; 29.47; 26.25; 26.11; 22.89; 14.30. $M_{calc} = 4065.00$ g mol^{-1} (100%) for $C_{272}H_{392}N_6O_{20}$; MS = 4069.94 g mol^{-1}.

20g. ^{1}H NMR (500 MHz, $CDCl_3$,), δ [ppm]: 7.80 (d; $J^3 = 7.8$ Hz; 8H); 7.48 (d; $J^3 = 7.8$ Hz; 8H); 7.42 (d; $J^3 = 8.6$ Hz; 8H); 7.39 (d; $J^3 = 8.6$ Hz; 8H); 7.03 (d; $J^3 = 1.4$ Hz; 4H); 6.98 (dd; $J^4 = 1.4$ Hz; $J^3 = 8.3$ Hz; 4H); 6.89−6.76 (m; 28H); 4.12−3.84 (m; 32H); 3.61−3.38 (m; 8H); 2.82−2.43 (m; 12H); 1.89−1.72 (m; 32H); 1.51−1.41 (m; 32H); 1.40−1.16 (m; 180H); 0.88 (t; $J^3 = 7.0$ Hz; 24H). ^{13}C NMR (125 MHz; $CDCl_3$), δ [ppm]: 167.18; 159.65; 158.73; 149.54; 149.10; 133.26; 131.50; 131.19; 130.41; 127.40; 127.09; 126.54; 126.47; 119.76; 114.82; 114.71; 114.37; 112.02; 92.17; 87.42; 69.61; 68.19; 31.96; 29.69; 29.50; 29.45; 29.38; 26.13; 26.11; 14.09. $M_{calc} = 4065.00$ g mol^{-1} (100%) for $C_{272}H_{392}N_6O_{20}$; MS = 4069.64 g mol^{-1}.

20h. ^{1}H NMR (200 MHz, $CDCl_3$), δ [ppm]: 7.84 (d; $J^3 = 8.0$ Hz; 8H); 7.64−7.32 (m; 24H); 7.05 (dd; $J^4 = 2.0$ Hz; $J^3 = 8.1$ Hz; 4H); 7.02(d; $J^4 = 2.0$ Hz; 4H); 6.73−6.72 (m; 20H); 4.10−3.81 (m; 32H); 3.67−3.32 (m; 8H); 2.72−2.35 (m; 12H); 2.00−1.62 (m; 32H); 1.57−1.07 (m; 212H); 0.88 (t; $J^3 = 68$ Hz; 24H). ^{13}C NMR (50 MHz; $CDCl_3$), δ [ppm]: 159.20; 149.63; 148.92; 133.43; 133.07; 124.91; 117.14; 116.74; 115.92; 114.69; 113.51; 112.33; 88.39; 88.02; 69.42; 68.26; 32.15; 29.92; 29.86; 29.64; 29.60; 29.43; 26.23; 22.91; 14.34. $M_{calc} = 4057.93$ g mol^{-1} (100%) for $C_{272}H_{384}N_6O_{20}$; MS = 4058.32 g mol^{-1}.

20i. ^{1}H NMR (500 MHz, $CDCl_3$), δ [ppm]: 7.82 (d; $J^3 = 8.2$ Hz; 8H); 7.65 (d; $J^3 = 8.2$ Hz; 8H); 7.56−7.39 (m; 24H); 6.91(d; $J^3 = 8.8$ Hz; 8H); 6.87−6.81 (m; 16H); 4.02−3.90 (m; 24H); 3.65−3.31 (m; 8H); 2.71−2.33 (m; 12H); 1.80−1.71 (m; 24H); 1.51−1.42 (m; 24H); 1.40−1.19 (m; 116H); 0.88 (t; $J^3 = 7$ Hz; 12H). ^{13}C NMR (125 MHz, $CDCl_3$), δ [ppm]: 168.59; 159.53; 159.34; 148.96; 133.45; 131.84; 129.87; 129.63; 128.49; 115.71; 115.59; 114.86; 114.75; 92.96; 88.67; 88.34; 71.53; 71.32; 71.30; 71.26; 29.94; 29.88; 29.80; 29.74; 29.71; 29.87; 29.61; 29.53; 29.48; 29.41; 26.35; 22.84; 14.13. $M_{calc} = 3320.20$ g mol^{-1} (100%) for $C_{224}H_{288}N_6O_{16}$; MS = 3329.23 g mol^{-1}.

Acknowledgment. The work was supported by ESF/2007/03 grant. The X-ray diffraction measurements were accomplished at the Structural Research Laboratory, established with financial support from European Regional Development Found, Project WKP_ 1/1.4.3./1/2004/72/72/165/2005/U. S.B., B.D., and D.G. thank the Thai government, the ANR (DENDRIMAT), the CNRS, and the Université de Strasbourg for support and funding.

Supporting Information Available: Chemical synthetic details and spectroscopic characterization of the precursory compounds, the complete experimental methods, and comparative phase diagrams of acids and dendrimers. This material is available free of charge via the Internet at http://pubs.acs.org.

References and Notes

(1) Kirsh, P.; Bremer, M. *Angew. Chem., Int. Ed.* **2000**, *39*, 4216–4235.
(2) (a) O'Neill, M.; Kelly, S. M. *Adv. Mater.* **2003**, *15*, 1135–1146. (b) Laschat, S.; Baro, A.; Steinke, N.; Giesselmann, F.; Hugele, C.; Scalia, G.; Judele, R.; Kapatsina, E.; Sauer, S.; Schreivogel, A.; Tosoni, M. *Angew. Chem., Int. Ed.* **2007**, *46*, 4832–4887. (c) Sergeyev, S.; Pisulab, W.; Geerts, Y. H. *Chem. Soc. Rev.* **2007**, *36*, 1902–1929. (d) Shimizu, Y.; Oikawa, K.; Nakayama, K.; Guillon, D. *J. Mater. Chem.* **2007**, *17*, 4223–4229.
(3) (a) Kato, T.; Mizoshita, N.; Kishimoto, K. *Angew. Chem., Int. Ed.* **2006**, *45*, 38–68. (b) Kato, T.; Yasuda, T.; Kamikawa, Y.; Yoshio, M. *Chem. Commun.* **2009**, 729–739.
(4) Bruce, D. W., Coles, H. J., Goodby, J. W., Sambles, J. R., Eds. *Philos. Trans. R. Soc. London A* **2006**, *364*, 2565−2843.
(5) Goodby, J. W.; Saez, I. M.; Cowling, S. J.; Görtz, V.; Draper, M.; Hall, A. W.; Sia, S.; Cosquer, G.; Lee, S. E.; Raynes, E. P. *Angew. Chem., Int. Ed.* **2009**, *47*, 2754–2787.
(6) (a) Deschenaux, R.; Goodby, J. W. In *Ferrocenes: Homogeneous Catalysis, Organic Synthesis, Materials Sciences*; Togni, A., Hayashi, T., Eds.; VCH: Weinheim, 1995; Chapter 9, pp 471−495. (b) Binnemans, K.; Görller-Walrand, C. *Chem. Rev.* **2002**, *102*, 2303–2345. (c) Donnio, B.; Guillon, D.; Bruce, D. W.; Deschenaux, R. In *Metallomesogens*; McCleverty, J. A., Meyer, T. J., Eds.; Comprehensive Coordination Chemistry II: From Biology to Nanotechnology; Elsevier: Oxford, UK, 2003; Vol. *7*, Chapter 7.9, pp 357−627.
(7) Binnemans, K. *Chem. Rev.* **2005**, *105*, 4148–4204.
(8) (a) Lee, M.; Cho, B.-K.; Zin, W.-C. *Chem. Rev.* **2001**, *101*, 3869–3892. (b) Lee, M.; Yoo, Y.-S. *J. Mater. Chem.* **2002**, *12*, 2161–2168. (c) Lim, Y.-b.; Moon, K.-Y.; Lee, M. *J. Mater. Chem.* **2008**, *18*, 2909–2918.
(9) Nguyen, H.-T.; Destrade, C.; Malthête, J. *Adv. Mater.* **1997**, *9*, 375–388.
(10) Demus, D. *Liq. Cryst.* **1989**, *5*, 75–110.
(11) (a) Tschierske, C. *Annu. Rep. Prog. Chem., Sect. C* **2001**, *97*, 191–267. (b) Tschierske, C. *Chem. Soc. Rev.* **2007**, *36*, 1930–1970.
(12) (a) Peltz, G.; Diele, S.; Weissflog, W. *Adv. Mater.* **1999**, *11*, 707–724. (b) Reddy, R. A.; Tschierske, C. *J. Mater. Chem.* **2006**, *16*,

907–961. (c) Takezoe, H.; Kishikawa, K.; Gorecka, E. *J. Mater. Chem.* **2006**, *16*, 2412–2416.
(13) (a) Metrangolo, P.; Neukirch, H.; Pilati, T.; Resnati, G. *Acc. Chem. Res.* **2005**, *38*, 386–395. (b) Metrangolo, P.; Meyer, F.; Pilati, T.; Resnati, G.; Terraneo, G. *Angew. Chem., Int. Ed.* **2008**, *47*, 6114–6127.
(14) (a) Tschierske, C. *Prog. Polym. Sci.* **1996**, *21*, 775–852. (b) Paleos, C. M.; Tsiourvas, D. *Liq. Cryst.* **2001**, *28*, 1127–1161.
(15) *Handbook of Liquid Crystals*; Demus, D., Goodby, J. W., Gray, G. W., Spiess, H.-W., Vill, V., Eds.; Wiley-VCH: Weinheim, 1998.
(16) (a) Ajay Mallia, V.; Tamaoki, N. *Chem. Soc. Rev.* **2004**, *33*, 76–84. (b) Imrie, C. T.; Henderson, P. A. *Chem. Soc. Rev.* **2007**, *36*, 2096–2124. (c) Yelamaggad, C. V.; Achalkumar, A. S.; Shankar Rao, D. S.; Prasad, S. K. *Org. Lett.* **2007**, *9*, 2641–2644. (d) Bialecka-Florjanczyk, E.; Sledzinska, I.; Gorecka, E.; Przedmojski, J. *Liq. Cryst.* **2008**, *35*, 401–406. (e) Yelamaggad, C. V.; Shanker, G.; Hiremath, U. S.; Prasad, S. K. *J. Mater. Chem.* **2008**, *18*, 2927–2949. (f) Aldred, M. P.; Hudson, R.; Kitney, S. P.; Vlachos, P.; Liedtke, A.; Woon, K. L.; O'Neill, M.; Kelly, S. M. *Liq. Cryst.* **2008**, *35*, 413–427.
(17) (a) Newkome, G. R.; Moorefield, C. N.; Vögtle, F. In *Dendrimers and Dendrons: Concepts, Synthesis and Applications*; Wiley & Sons: Weinheim, Germany, 2001. (b) Fréchet, J. M. J., Tomalia, D. A., Eds. In *Dendrimers and other Dendritic Polymers*; Wiley Series in Polymer Science; Wiley& Sons: Chichester, 2001.
(18) (a) Krówczyński, A.; Górecka, E.; Pociecha, D.; Szydłowska, J.; Przedmojski, J. *Liq. Cryst.* **1996**, *20*, 607–610. (b) Jeong, K.-U.; Jing, A. J.; Monsdorf, B.; Graham, M. J.; Harris, F. W.; Cheng, S. Z. D. *J. Phys. Chem. B* **2007**, *111*, 767–777. (c) Mamlouk, H.; Heinrich, B.; Bourgogne, C.; Donnio, B.; Guillon, D.; Felder-Flesch, D. *J. Mater. Chem.* **2007**, *17*, 2199–2205. (d) Zelcer, A.; Donnio, B.; Bourgogne, C.; Cukiernik, F. D.; Guillon, D. *Chem. Mater.* **2007**, *19*, 1992–2006. (e) Yoshizawa, A. *J. Mater. Chem.* **2008**, *18*, 2877–2889. (f) Pal, S. K.; Kumar, S.; Seth, J. *Liq. Cryst.* **2008**, *35*, 521–525. (g) Kouwer, P. H. J.; Mehl, G. H. *J. Mater. Chem.* **2009**, *19*, 1564–1575.
(19) (a) Goodby, J. W.; Mehl, G. H.; Saez, I. M.; Tuffin, R. P.; Mackenzie, G.; Auzély-Velty, R.; Benvegnu, T.; Plusquellec, D. *Chem. Commun.* **1998**, 2057–2070. (b) Saez, I. M.; Goodby, J. W. *J. Mater. Chem.* **2005**, *15*, 26–40. (c) Saez, I. M.; Goodby, J. W. *Struct. Bonding* (*Berlin*) **2008**, *128*, 1–62.
(20) Donnio, B.; Guillon, D. *Adv. Polym. Sci.* **2006**, *201*, 45–155.
(21) (a) Balagurusamy, V. S. K.; Ungar, G.; Percec, V.; Johansson, G. *J. Am. Chem. Soc.* **1997**, *119*, 1539–1555. (b) Percec, V.; Cho, W. D.; Möller, M.; Prokhorova, S. A.; Ungar, G.; Yeardley, D. J. P. *J. Am. Chem. Soc.* **2000**, *122*, 4249–4250. (c) Percec, V.; Cho, W. D.; Ungar, G.; Yeardley, D. J. P. *Angew. Chem., Int. Ed.* **2000**, *39*, 1597–1602.
(22) (a) Kato, T.; Matsuoka, T.; Nishii, M.; Kamikawa, Y.; Kanie, K.; Nishimura, T.; Yashima, E.; Ujiie, S. *Angew. Chem., Int. Ed.* **2004**, *43*, 1969–1972. (b) Kamikawa, Y.; Kato, T. *Org. Lett.* **2006**, *8*, 2463–2466. (c) Percec, V.; Holerca, M. N.; Nummelin, S.; Morrison, J. J.; Glode, M.; Smidrkal, J.; Peterca, M.; Rosen, B. M.; Uchida, S.; Balagurusamy, V. S. K.; Sienkowska, M. J.; Heiney, P. A. *Chem.—Eur. J.* **2006**, *12*, 6216–6241. (d) Percec, V.; Peterca, M.; Sienkowska, M. J.; Ilies, M. A.; Aqad, E.; Smidrkal, J.; Heiney, P. A. *J. Am. Chem. Soc.* **2006**, *128*, 3324–3334.
(23) (a) Percec, V.; Glodde, M.; Johansson, G.; Balagurusamy, V. S. K.; Heiney, P. A. *Angew. Chem., Int. Ed.* **2003**, *42*, 4338–4342. (b) Percec, V.; Mitchell, C. M.; Cho, W.-D.; Uchida, S.; Glodde, M.; Ungar, G.; Zeng, X.; Liu, Y.; Balagurusamy, V. S. K.; Heiney, P. A. *J. Am. Chem. Soc.* **2004**, *126*, 6078–6094. (c) Percec, V.; Imam, M. R.; Bera, T. K.; Balagurusamy, V. S. K.; Peterca, M.; Heiney, P. A. *Angew. Chem., Int. Ed.* **2005**, *44*, 4739–4745. (d) Percec, V.; Glodde, M.; Peterca, M.; Rapp, A.; Schnell, I.; Speiss, H. W.; Bera, T. K.; Miura, Y.; Balagurusamy, V. S. K.; Aqad, E.; Heiney, P. A. *Chem.—Eur. J.* **2006**, *12*, 6298–6314. (e) Percec, V.; Won, B. C.; Peterca, M.; Heiney, P. A. *J. Am. Chem. Soc.* **2007**, *129*, 11265–11278. (f) Percec, V.; Smidrkal, J.; Peterca, M.; Mitchell, C. M.; Nummelin, S.; Dulcey, A. E.; Sienkowska, M. J.; Heiney, P. A. *Chem.—Eur. J.* **2007**, *13*, 3989–4007. (g) Percec, V.; Imam, M. R.; Peterca, M.; Wilson, D. A.; Heiney, P. A. *J. Am. Chem. Soc.* **2009**, *131*, 1294–1304.
(24) (a) Ponomarenko, S. A.; Boiko, N. I.; Shibaev, V. P. *J. Polym. Sci. C* **2001**, *43*, 1–45. (b) Guillon, D.; Deschenaux, R. *Curr. Opin. Solid State Mater. Sci.* **2002**, *6*, 515–525. (c) Donnio, B.; Buathong, S.; Bury, I.; Guillon, D. *Chem. Soc. Rev.* **2007**, *36*, 1495–1513. (d) Deschenaux, R.; Donnio, B.; Guillon, D. *New J. Chem.* **2007**, *31*, 1064–1073.
(25) Li, J.-f.; Crandall, K. A.; Chu, P.; Percec, V.; Petschek, R. G.; Rosenblatt, C. *Macromolecules* **1996**, *29*, 7813–7819.
(26) (a) Gehringer, L.; Guillon, D.; Donnio, B. *Macromolecules* **2003**, *36*, 5593–5601. (b) Gehringer, L.; Bourgogne, C.; Guillon, D.; Donnio, B. *J. Am. Chem. Soc.* **2004**, *126*, 3856–3867. (c) Gehringer, L.; Bourgogne, C.; Guillon, D.; Donnio, B. *J. Mater. Chem.* **2005**, *15*, 1696–1703. (d) Buathong, S.; Gehringer, L.; Donnio, B.; Guillon, D. *C. R. Chim.* **2009**, *12*, 138–162.
(27) (a) Campidelli, S.; Lenoble, J.; Barbera, J.; Paolucci, F.; Marcaccio, M.; Paolucci, D.; Deschenaux, R. *Macromolecules* **2005**, *38*, 7915–7925. (b) Campidelli, S.; Vazquez, E.; Milic, D.; Lenoble, J.; Atienza Castellanos, C.; Sarova, G.; Guldi, D. M.; Deschenaux, R.; Prato, M. *J. Org. Chem.* **2006**, *71*, 7603–7610. (c) Lenoble, J.; Campidelli, S.; Maringa, N.; Donnio, B.; Guillon, D.; Yevlampieva, N.; Deschenaux, R. *J. Am. Chem. Soc.* **2007**, *129*, 9941–9952.
(28) *Transition Metals in Organic Synthesis: A Practical Approach*; Gibson, S. E., Ed.; Oxford University Press: New York, 1997.
(29) Mitsunobu, O. *Synthesis* **1981**, 1–28.
(30) Corey, E. J.; Fuchs, P. L. *Tetrahedron Lett.* **1972**, 3769–3772.
(31) V_{mol} is the molecular volume, and S, for the Col_h, is defined as $S = a^2\sqrt{3}/2$. Similarly, for Col_r and Col_o, $S = {}^1/_2ab$ and ${}^1/_2ab$ sin γ, respectively.
(32) Gray, G. W.; Goodby, J. W. In *Smectic Liquid Crystals; Textures and Structures*; Leonard Hill: Glasgow, 1984.
(33) (a) *International Tables for Crystallography*, 4th ed.; Hahn, T., Ed.; The International Union of Crystallography; Kluwer Academic: Dordrecht, 1995; Vol. *A*. (b) Hammond, C. In *The Basics of Crystallography and Diffraction*, 2nd ed.; IUCr, Oxford Science Publications: Oxford, 2001.
(34) (a) Serrano, J. L.; Sierra, T. *Coord. Chem. Rev.* **2003**, *242*, 73. (b) Vera, F.; Serrano, J. L.; Sierra, T. *Chem. Soc. Rev.* **2009**, *38*, 781–796.
(35) Donnio, B.; Heinrich, B.; Gulik-Krzywicki, T.; Delacroix, H.; Guillon, D.; Bruce, D. W. *Chem. Mater.* **1997**, *9*, 2951–2965.
(36) Morale, F.; Date, R. W.; Guillon, D.; Bruce, D. W.; Finn, R. L.; Wilson, C.; Blake, A. J.; Schröder, M.; Donnio, B. *Chem.—Eur. J.* **2003**, *9*, 2484–2501.
(37) Levelut, A. M. *J. Chim. Phys.* **1983**, *80*, 149–161.